Influence of Reinforcement on the Loading Capacity of Geopolymer Concrete Pipe

S. Dangol, J. Li, V. Sirivivatnanon, and P. Kidd

Abstract Geopolymer concrete is emerging as a sustainable construction material due to utilization of industrial by-products, which greatly reduces its carbon footprint. Past studies of the mechanical properties and resistance to sulfuric acid reaction of cement-less geopolymer concrete indicated its suitability for precast concrete pipes over ordinary Portland cement (OPC) concrete. In the present study, a three-dimensional finite element (FE) model of reinforced concrete pipe was developed using commercial software ANSYS-LSDYNA. The load-carrying capacity of reinforced and non-reinforced geopolymer concrete pipes under the three-edge bearing (TEB) test was investigated and compared with OPC concrete pipes. The results indicated geopolymer concrete with comparable compressive strength to OPC concrete showed higher loading capacity in a pipe structure due to its better tensile performance. The effect of steel reinforcement area on the loading capacity of geopolymer concrete pipes was quantitatively analyzed, and they met the specified strength requirement for OPC concrete in the ASTM standard, with up to 20% reduction in the reinforcement area.

Keywords Geopolymer concrete pipe · Pipe loading capacity · Numerical modelling

1 Introduction

As an integral part of civil infrastructure, concrete pipes are used as conduit for sewage and storm water. Ordinary Portland cement (OPC) concrete pipes have demonstrated reliable long-term performance over years of usage. Their structural

S. Dangol · J. Li (✉) · V. Sirivivatnanon
School of Civil and Environmental Engineering, University of Technology Sydney, Sydney, NSW, Australia
e-mail: jun.li-2@uts.edu.au

P. Kidd
Cement Australia Pty. Ltd., Brisbane, QLD, Australia

W. Duan et al. (eds.), *Nanotechnology in Construction for Circular Economy*,
Lecture Notes in Civil Engineering 356,
https://doi.org/10.1007/978-981-99-3330-3_18

performance is evaluated in terms of test load (D_{peak}) corresponding to load causing a 0.3 mm crack and by ultimate load (D_{ult}) corresponding to the load supported before failure of the pipe. The three-edge bearing (TEB) test is a standardized test described in AS/NZS-4058 [1] and ASTM-C76M [2] to examine the mechanical strength of a pipe, wherein a line load is applied to the crown of the pipe while the base of the pipe is supported by two bearers. However, carrying out such destructive tests is uneconomical and often inefficient, considering the need for human judgement of crack formation during the TEB test. Hence, numerous researchers have performed numerical modelling of concrete pipes to investigate the load-carrying capacity and load–deflection behavior of concrete pipes.

de la Fuente et al. [3] and de Figueiredo et al. [4] simulated the TEB test for steel fiber-reinforced concrete (SFRC) pipe using a MAP (mechanical analysis of pipes) model to study mechanical behavior. The results from the numerical simulation were compared with experimental results, concluding the efficiency of the numerical model to design fiber-reinforced concrete pipes because the model gave an average error of 7%, which was within the anticipated contingency. Similarly, Ferrado et al. [5] used the commercial software ABAQUS to simulate SFRC pipes. In their study, the behavior of the pipes was defined by compression and the uniaxial tension curve based on theoretical formulation in the existing literature. The load–deflection curve and stress distribution of the pipes from experimental and numerical analysis were found to be in good agreement. Likewise, a numerical modelling of concrete pipes with different diameter and reinforcement configuration, was conducted by Younis et al. [6] to predict the service load and ultimate load. Following the concrete damage plasticity (CDP) model equation developed by Alfarah et al. [7], the non-linear behavior of concrete in compression and tension was defined. Based on their analysis and experimental results, the average prediction error was ≈6% for both service load and ultimate load, suggesting the reliability of numerical modelling for designing concrete pipes.

With the growing interest in sustainable construction materials, numerous studies of geopolymer concrete have been carried out, because it utilizes industrial by-product as its source material. Geopolymer is a cement-less binder formed as a result of reaction between aluminosilicate compounds with alkali [8–10]. Studies exploring the material properties of geopolymer concrete have shown significant development of strength at early age when cured at elevated temperature, high compressive strength, high flexural strength, and resistance to chemical attack [8, 11, 12]. Results of studies conducted to investigate indirect tensile strength and flexural strength of geopolymer have also showed higher indirect tensile strength and flexural strength in comparison with OPC concrete of the same compressive strength [13–16]. It is reported that the geopolymer possessed 1.4- and 1.6-fold higher value for indirect tensile strength and flexural strength, respectively, compared with OPC concrete [17]. Such properties of geopolymer concrete can be used to test the strength of pipes with reduced reinforcement bars. Although much efforts has been made to study the structural behavior of OPC SFRC to enhance the load-carrying capacity, study of the structural performance of geopolymer concrete pipes has not been carried out.

We investigated the load-carrying capacity of geopolymer concrete pipes based on a three-dimensional (3D) finite element (FE) model developed to simulate the TEB test. For this study, fly ash (FA)/slag-based powder form geopolymer Geocem^{TM} developed by Cement Australia with different ratio of FA and slag was utilized. The general purpose geopolymer binder we termed "geocem 1" contained 50% of FA and 32% of ground granulated blast-furnace slag (GGBFS), and the high strength geopolymer binder termed "geocem 2" comprised 30% FA and 50% GGBFS. The developed FE model was updated for both types of geopolymer concrete based on their mechanical properties. Subsequently, the FE model was used to evaluate the load-carrying capacity of the geopolymer pipes and the effect of reduced reinforcement area was evaluated.

2 FE Modelling of TEB Test

Our 3D FE model to simulate the TEB test for the pipe was based on commercial software ANSYS LS-DYNA (Fig. 1). The model comprised three components: concrete part, reinforcement steel bars, and bearing strips. Pipe of diameter 450 mm, length 1000 mm, and wall thickness of 42 mm were modelled. The concrete pipe and bearing strips were modelled using a 3D solid element (SOLID164). Similarly, a beam element (BEAM161) was used to model the reinforcing steel bars. Discrete steel formulation was used and perfect bond condition between the reinforcement bar and concrete was assumed. The bearing strips were modelled to mimic the boundaries in the TEB test: the lower bearing strips were fixed at the bottom to prevent translational and rotational degrees of freedom, and the upper bearing strips were restricted in all directions except for vertical displacement movement to allow for displacement-controlled loading on the pipe. The interaction between the pipe and the bearing strips was defined by an automatic contact surface. For the simulation of the test, displacement-controlled loading was defined as applied downward displacement on the upper bearer. The load–deflection curve was obtained for the analyzed pipe and is presented in terms of design load (N/m/mm) as specified in ASTM-C76M [2] and deflection in millimeters.

3 Material Modelling

Due to the complex material behavior of concrete, which includes elastic, non-linear plastic behavior, and material damage, the available concrete damage models for numerical modelling of concrete structures are often quite complex because these material models often contain parameters for which values are difficult to obtain from simple tests or have only mathematical meaning and no physical meaning [18]. To date, there are a lot of material models available to simulate concrete damage behavior [19, 20]. Among them, one simple concrete damage model implemented in

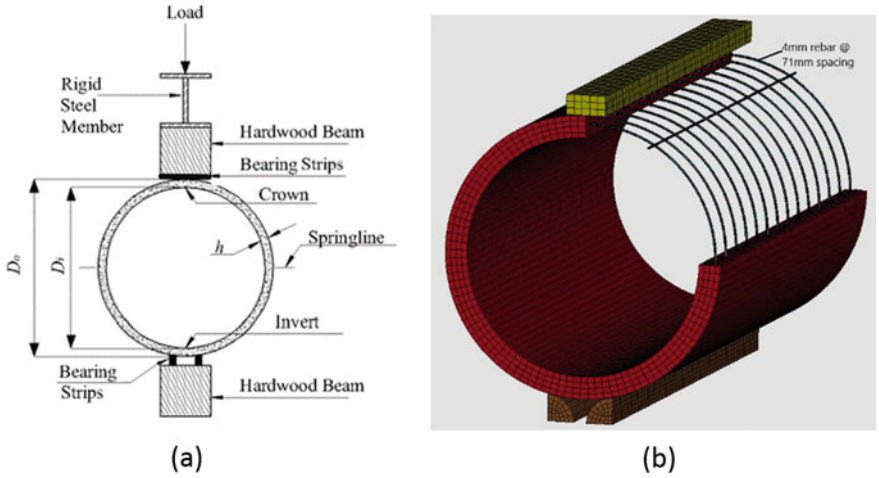

Fig. 1 **a** Three-edge bearing (TEB) test setup; **b** finite element model of concrete pipe for TEB test simulation

LS-DYNA to model concrete behavior is the Karagozian and Case (K&C) concrete model (Fig. 2). A key merit of the K&C concrete model for numerical simulation of concrete behavior is its reliance on just one main input parameter of unconfined compressive strength. Schwer & Malvar [21] stated that the K&C concrete model can be utilized for analysis involving new concrete materials with no detailed information available to characterize the concrete beside its compressive strength, owing to the fact that the unconfined compressive strength of the concrete not only describes the elastic response, but also accounts for the plastic response including shear failure, compression, and tensile failure.

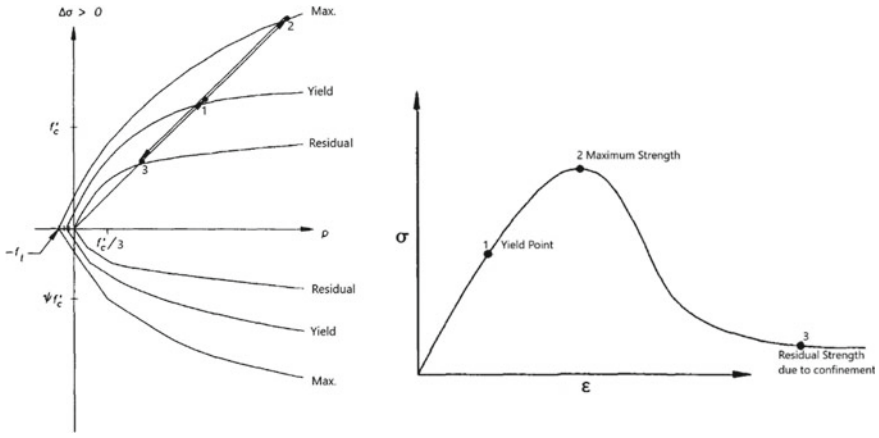

Fig. 2 Three failure surface of K&C concrete model [22]

The material constitutive behavior of the K&C concrete model comprises three parts; for initial loading, the stress is elastic until it reaches the yielding point, after which it increases further till the limit surface, called the maximum yield surface. Following the maximum yield surface, perfectly plastic, or softening behavior up to the residual yield surface is observed. These shear failure surfaces are mutually independent and can be formulated as [22, 23]:

$$F_i(p) = a_{0i} + \frac{p}{a_{1i} + a_{2i}\, p} \tag{1}$$

where i stands for either yield strength surface (y), maximum strength surface (m) or residual strength surface (r), p is the pressure calculated as $\frac{-I_1}{3}$, and the variables a_{ji} ($j = 0, 1, 2$) are the parameters calibrated from test data.

The resulting failure surface is interpolated between the maximum strength surface and either the yield surface or the residual strength surface as per the following equations:

$$F(I_1, J_2, J_3) = r(J_3)\left[\eta(\lambda)\left(F_m(p) - F_y(p)\right) + F_y(p)\right] \text{ for } \lambda \leq \lambda_m \tag{2}$$

$$= r(J_3)[\eta\,(\lambda)\,(F_m(p) - F_r(p)) + F_r(p)] \text{ for } \lambda \geq \lambda_{\mathrm{m}} \tag{3}$$

where I_1, J_2, and J_3 are the first, second, and third invariants of deviatoric stress tensor, λ is the modified effective plastic strain or the internal damage parameter, $\eta(\lambda)$ is the function of the internal damage parameter λ, with $\eta(0) = 0$, $\eta(\lambda_m) = 1$ and $\eta(\lambda \geq \lambda_m) = 0$, and $r(J_3)$ is the scale factor in the form of the William–Warnke equation [24].

The K&C concrete model considers the effect of strain rate, failure, and different mechanical–physical properties in compression and tension and hence is suitable for concrete modelling [18]. Based on the uniaxial compressive strength, material parameters are generated, requiring definition of only a few parameters for the functionality of the material model, and more parameters can be defined if required. The model requires 49 parameters to be defined, as well as equation of state, which is complicated because many parameters have only mathematical meaning. Hence, the developers advocate using parameter generation if the data to define the material are not available. The default parameters in the K&C concrete model were calibrated using uniaxial, biaxial, and tri-axial test data available for well characterized concrete and using the relationship such as tensile strength or modulus of elastic as the function of compressive strength [21]. Hence, the K&C concrete model was used for both OPC concrete and geopolymer concrete modelling for FE analysis (FEA).

For the reinforcement bar, an elastic–plastic constitutive relationship for reinforcement bar, with or without strain hardening, is commonly adopted for numerical analysis. However, the elastic-perfectly plastic assumption shown in Fig. 3a often fails to capture the steel stress at high strain, and accurate assessment of the strength

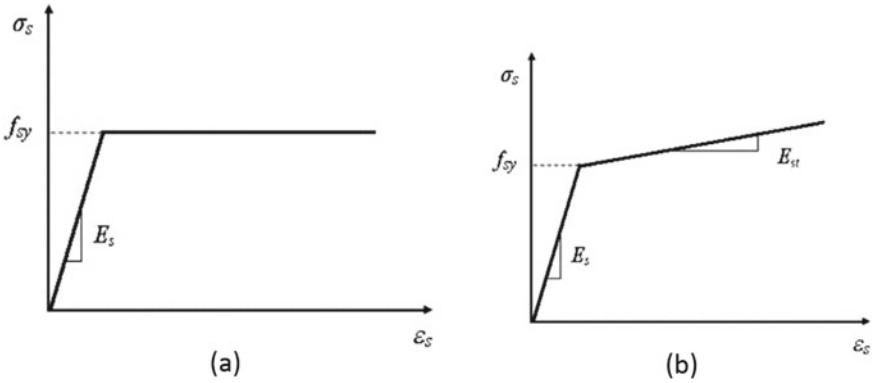

Fig. 3 Typical stress–strain curve of steel reinforcement representing **a** ideal elastic-perfectly plastic model; **b** bilinear elastic–plastic model with linear strain hardening [25]

of structure at large deformation cannot be made [26]. Hence, more accurate idealization of the stress–strain curve as shown in Fig. 3b was used. The Piecewise Linear Plasticity model used to represent the steel reinforcement behavior in LS-DYNA considers the plastic deformation, strain rate effects and failure [19]. In the Piecewise Linear Plasticity model, the stress–strain curve for the reinforcing steel is treated as bilinear by defining the tangent modulus [27]. The steel response is thus defined by parameters such as Young's modulus (E_s), yield strength (f_{sy}) and hardening modulus (E_{st}). The magnitude of E_{st} in the plastic regimen is commonly set at 1% of E_s [28, 29].

4 Load–Deflection Behavior of Concrete Pipes

A concrete pipe model was used for our study of the load–deflection behavior of geopolymer concrete pipes with respect to OPC concrete pipes. For the design of 450 mm reinforced concrete pipe, a reinforcement area of 175 mm^2/m was adopted based on minimum reinforcement area criteria for class II 450 mm concrete pipe defined in ASTM-C76M [2] in order to meet the design load criteria. Table 1 provides the details of the mechanical properties of the materials for the study based on the experimental results.

Comparing the results obtained from numerical analysis with the design requirement specified for OPC concrete of 50 N/m/mm and 75 N/m/mm for peak and ultimate load respectively in ASTM-C76M [2] with the geocem 1 and geocem 2 FEA results, it was evident from the load–deflection curve shown in Fig. 4 that the geopolymer concrete exhibited better load-carrying capacity than OPC concrete. The peak load and ultimate load value of the OPC pipe were 85 N/m/mm and 113 N/m/mm respectively, and for the geocem 1 and geocem 2 pipes, the peak load value was 100 N/m/mm and 105 N/m/mm and the ultimate load value was observed to be 119 N/m/

Table 1 Material properties of the pipe model

Material property	Geocem 1	Geocem 2	OPC
Compressive strength (MPa)	50	50	50
Tensile strength (MPa)	3.6	3.8	2.3
Poisson's ratio	0.2	0.2	0.2
Rebar yielding stress (MPa)	500	500	500

OPC, ordinary Portland cement

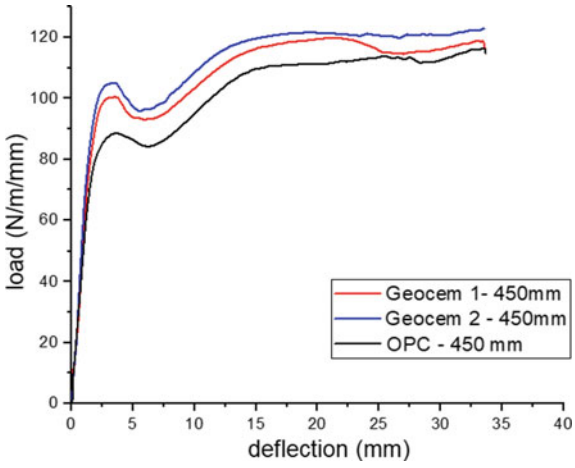

Fig. 4 Load–deflection curves of the 450 mm pipes

mm and 121 N/m/mm respectively. The load-carrying capacity of both geopolymer concretes outperformed the OPC concrete load requirement by ≈15% for peak load capacity and ≈5% for ultimate load capacity. The high tensile strength of geopolymer concrete benefited the load-bearing capacity of the pipe.

In the load–deflection plot of the pipe, a drop in the load was noticed after the pipe reached its peak load capacity. Such a drop in loading capacity for a single-cage model was also observed by Tehrani [30], Peyvandi et al. [31], and Younis et al. [6]. The rise in the load capacity following the drop after peak load signifies the load stress being carried by the steel reinforcement.

5 Effect of Change in Reinforcement Area

To investigate the effect of steel reinforcement area on the load–deflection behavior of the reinforced OPC, geocem 1 and geocem 2 concrete pipes, the steel reinforcement was reduced by 20%, 40% and 50% from the total reinforcement area. The main objective was to the test the load capacity in geopolymer concrete pipes under reduced

reinforcement and evaluate against the strength requirement as specified in ASTM-C76M [2].

Figure 5 shows the load–deflection plot of 450 mm pipes under reduced reinforcement conditions. It is obvious for both geopolymer concrete types (Fig. 5a, b) that the load-carrying capacity of the pipes decreased with the reduction in the reinforcement area, especially the ultimate load-carrying capacity. As the development of crack in concrete structures is dependent on the tensile strength of the concrete, changing the steel reinforcement does not change the service load capacity of the pipe, but alters the ultimate load capacity. When sufficient tensile stress develops in the concrete surface causing the concrete to crack, the pipe loses its capacity, which is marked by the drop in the load capacity. As the tensile stress in the concrete pipe is transferred to the steel reinforcement, regaining load capacity is observed until it reaches its ultimate load capacity, after which the pipe fails. With the reduction of reinforcement area by 40 and 50%, a significant reduction in the post-crack loading capacity of the pipe was observed; however, the reduction of reinforcement area by 20% showed decrease ultimate load capacity by 7% and 6% for geocem 1 and geocem 2, respectively, but still satisfied the design requirement specified in the ASTM standard. The strength gained by fully reinforced OPC concrete pipe was approximately equivalent to the strength gained by geopolymer concrete pipes with 20% reduced reinforcement area. This result suggested the geopolymer concrete pipes could resist load without failure with up to 20% reduction in the area of steel reinforcement.

Furthermore, in the comparative study of the load–deflection behavior of unreinforced OPC concrete pipe against unreinforced geocem 1 concrete pipe shown in Fig. 5c, the test load capacity of the unreinforced OPC concrete pipe was 69 N/m/mm and the test load capacity of geocem 1 was 96 N/m/mm. AS/NZS-4058 specifies the test load for 450 mm unreinforced concrete pipe as 30 KN/m (or 67 N/m/mm) [1]. The load capacity of the geocem 1 pipe was 37% higher than that of the OPC concrete pipe. Moreover, considering the AS/NZS-4058 requirement of 67 N/m/mm as the test load and 100 N/m/mm as the ultimate load capacity for class 3 reinforced 450 mm concrete pipe [1], unreinforced geopolymer concrete pipe can be used to meet the design requirement of class 3 reinforced concrete pipe.

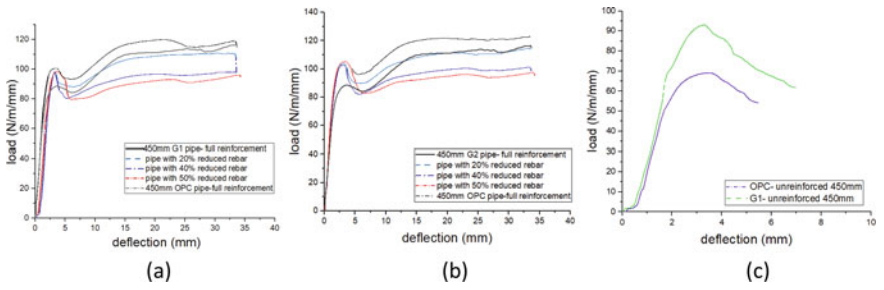

Fig. 5 a–c Effect on load–deflection behavior of 450 mm pipes due to change in reinforcement steel area

6 Conclusion

We developed a 3D FE model of 450 mm concrete pipe to simulate the TEB test in LS-DYNA. The K&C concrete model was used to characterize the OPC and geopolymer concrete behavior, and a bilinear elastic–plastic model with linear strain hardening was used to model steel reinforcement in the pipe FE model. In the comparative analysis of geopolymer and OPC concrete pipes, the peak load and ultimate load capacity exhibited by both types of geopolymer concrete pipes were noticeably higher than by OPC concrete pipe, which can be attributed to the high tensile strength of geopolymer concrete. The FE model was used to study the effect of changing the reinforcement area on the load-carrying capacity of geopolymer and OPC concrete pipes. The change in steel reinforcement area affected the post-crack behavior of the pipes, because reinforcement mostly contributes to strength development in cracked concrete sections. Based on the numerical study, the reinforcement bar area in concrete pipes can be reduced by 20% and still meet the specified design load criteria. Further, comparing the loading capacity of unreinforced geopolymer concrete pipe against OPC concrete pipe revealed that the unreinforced geopolymer concrete pipe can satisfy the load criteria for AS/NZS class 3 450 mm reinforced concrete pipe. Thus, with the use of geopolymer concrete, reinforcement requirement for concrete pipe can be reduced to a certain percentage and still meet the specified design load criteria.

Acknowledgements This research was funded through an Australian Research Council Research Hub for Nanoscience Based Construction Materials Manufacturing (NANOCOMM) with the support of Cement Australia. The authors are grateful for the financial support of the Australian Research Council (IH150100006) in conducting this study.

References

1. AS/NZS-4058 (2007) Precast concrete pipes (pressure and non-pressure). Standards Australia Sydney, NSW
2. ASTM-C76M (2019) Standard specification for reinforced concrete culvert, storm drain, and sewer pipe (Metric) 1
3. de la Fuente A, de Figueiredo AD, Aguado A, Molins C, Neto PJC (2011) Experimentation and numerical simulation of steel fibre reinforced concrete pipes. Mater Constr 61(302):275–288
4. de Figueiredo A, Aguado A, Molins C, Chama Neto PJ (2012) Steel fibre reinforced concrete pipes. Part 2: numerical model to simulate the crushing test. Revista IBRACON de Estruturas e Materiais 5(1):12–25
5. Ferrado FL, Escalante MR, Rougier VC (2018) Simulation of the three edge bearing test: 3D model for the study of the strength capacity of SFRC pipes. Mecánica Computacional 36(6):195–204
6. Younis A-A, Shehata A, Ramadan A, Wong LS, Nehdi ML (2021) Modeling structural behavior of reinforced-concrete pipe with single, double and triple cage reinforcement. Eng Struct 240:112374
7. Alfarah B, López-Almansa F, Oller S (2017) New methodology for calculating damage variables evolution in plastic damage model for RC structures. Eng Struct 132:70–86

8. Davidovits J (1991) Geopolymers: inorganic polymeric new materials. J Therm Anal Calorim 37(8):1633–1656
9. Habert G, De Lacaillerie JDE, Roussel N (2011) An environmental evaluation of geopolymer based concrete production: reviewing current research trends. J Clean Prod 19(11):1229–1238
10. Provis JL, van Deventer JSJ (2014) Alkali activated materials. Springer, Dordrecht
11. Abdullah M, Hussin K, Bnhussain M, Ismail K, Ibrahim W (2011) Mechanism and chemical reaction of fly ash geopolymer cement-A review. Int J Pure Appl Sci Technol 6(1):35–44
12. Wallah S, Rangan BV (2006) Low-calcium fly ash-based geopolymer concrete: long-term properties
13. Hardjito D, Rangan BV (2005) Development and properties of low-calcium fly ash-based geopolymer concrete
14. Neupane K, Chalmers D, Kidd P (2018) High-strength geopolymer concrete—properties, advantages and challenges. Adv Mater 7:15–25
15. Ramujee K, PothaRaju M (2017) Mechanical properties of geopolymer concrete composites. Mater Today: Proc 4(2, Part A):2937–45
16. Sofi M, van Deventer JSJ, Mendis PA, Lukey GC (2007) Engineering properties of inorganic polymer concretes (IPCs). Cem Concr Res 37(2):251–257
17. Raijiwala D, Patil H (2011) Geopolymer concrete: a concrete of the next decade. Concrete solutions, vol 287
18. Kral P, Hradil P, Kala J, Hokes F, Husek M (2017) Identification of the parameters of a concrete damage material model. Procedia Eng 172:578–585
19. Abedini M, Zhang C (2021) Performance assessment of concrete and steel material models in LS-DYNA for enhanced numerical simulation, a state of the art review. Arch Comput Methods Eng 28(4):2921–2942
20. Xu M, Wille K (2015) Calibration of K&C concrete model for UHPC in LS-DYNA. Adv Mater Res (Trans Tech Publ) 1081:254–259
21. Schwer LE, Malvar LJ (2005) Simplified concrete modeling with* MAT_CONCRETE_ DAMAGE_REL3. JRI LS-Dyna User Week, pp 49–60
22. Malvar LJ, Crawford JE, Wesevich JW, Simons D (1997) A plasticity concrete material model for DYNA3D. Int J Impact Eng 19(9–10):847–873
23. Wu Y, Crawford JE, Magallanes JM (2012) Performance of LS-DYNA concrete constitutive models. In: 12th international LS-DYNA users conference, vol 1, pp 1–14
24. Chen W-F, Han D-J (1988) Plasticity for structural engineers. Springer-Verlag, New York
25. Du X, Jin L (2021) Methodology: meso-scale simulation approach. In: Size effect in concrete materials and structures, Springer, pp 27–76
26. Supaviriyakit T, Pornpongsaroj P, Pimanmas A (2004) Finite element analysis of FRP-strengthened RC beams. Songklanakarin J Sci Technol 26(4):497–507
27. LSTC (2014) LS-DYNA keyword user's manual: material models. In: LS-DYNA R7.1 edn, vol II. Livermore Software Technology Corporation, Livermore, CA
28. Elnashai AS, Izzuddin BA (1993) Modelling of material non-linearities in steel structures subjected to transient dynamic loading. Earthquake Eng Struct Dynam 22(6):509–532
29. Xiao S (2015) Numerical study of dynamic behaviour of RC beams under cyclic loading with different loading rates. Mag Concr Res 67(7):325–334
30. Tehrani AD (2016) Finite element analysis for ASTM C-76 reinforced concrete pipes with reduced steel cage
31. Peyvandi A, Soroushian P, Jahangirnejad S (2013) Enhancement of the structural efficiency and performance of concrete pipes through fiber reinforcement. Constr Build Mater 45:36–44